Electrical reliability and leakage mechanisms in highly resistive multiferroic La$_{0.1}$Bi$_{0.9}$FeO$_3$ ceramics

S. Y. Wang,[1,2,a)] Xue Qiu,[1] J. Gao,[2] Yu Feng,[1] W. N. Su,[1] J. X. Zheng,[1] D. S. Yu,[1] and D. J. Li[1]

[1]*College of Physics and Electronic Information Science, Tianjin Normal University, Tianjin 300074, People's Republic of China*
[2]*Department of Physics, The University of Hong Kong, Pokfulam Road, Hong Kong*

Multiferroic La$_{0.1}$Bi$_{0.9}$FeO$_3$ (LBFO) ceramics with high resistivity were synthesized by using a modified rapid thermal process. The LBFO ceramics show very low leakage and low dielectric loss. Well saturated ferroelectric hysteresis loops and polarization switching currents have been observed. For a maximum applied electric field of 145 kV/cm, the remanent polarization is 17.8 μC/cm^2 and the coercive filed is 75 kV/cm. The dominant conduction mechanism in the LBFO ceramics has been found to be the space-charge-limited current mechanism rather than the thermal excitation mechanism. Electrical reliability related to the fatigue and polarization retention of the LBFO ceramics has also been discussed with the leakage mechanisms. © *2011 American Institute of Physics*. [doi:10.1063/1.3580604]

BiFeO$_3$ (BFO) with perovskite structure has attracted much attention for a long time, because its high ferroelectric Curie temperature and antiferromagnetic Neel temperature is advantageous for potential application in functional devices.[1–4] Theoretical studies using density function theory predict a large ferroelectric polarization of 90–100 μC/cm^2 in BFO.[5] However, such a large polarization was only observed in BFO thin films and single crystals.[6,7] In ceramic samples, the measured polarization values are relatively low. At room temperature a remanent polarization of 11.7 μC/cm^2 was obtained in a quenched BiFeO$_3$ ceramic,[8] a value of 15.5 μC/cm^2 was obtained in a quenched Bi$_{0.95}$La$_{0.05}$FeO$_3$ ceramic,[9] and a value of 23 μC/cm^2 was obtained in a high-pressure synthesized BiFeO$_3$ ceramic.[10] It has been pointed out that the difficulty in obtaining a well saturated polarization loops (P-E) and large remanent polarization comes from the large leakage current at room temperature, probably due to the presence of defects and impurities in the BFO ceramics.[8–11]

The requirements for the application of ferroelectric BFO in future devices include not only larger remanent polarization but also electrical reliability that is related to fatigue and long-term data retention. Because of pyroelectric and piezoelectric properties of the BFO ceramics,[11,12] the electric cycling can induce heating effect and mechanical stresses that degrade the material, which is generally called the fatigue of the material. On the other hand, the polarization retention loss (the decrease in the remanent polarization with the elapsed time in the absence of an external electric field) is also a crucial factor that needs investigation.

The ferroelectric polarization and electrical reliability are strongly deteriorated by the leakage currents.[4,13] The knowledge of the leakage current in the BFO ceramics is of fundamental interest to understand the ferroelectric performance and electrical reliability. As an added bonus, such knowledge also allows for the characterization of the injection mechanism of charge carriers from the electrode into the materials.[14–16] So far, this information has been gathered mostly in thin film and single crystal of BFO.[2,4,14] Although Yuan et al.[11] proposed the Poole–Frenkel conduction mechanism to be the controlling mechanism in Nd-doped BFO ceramics, Ramachandran et al.[15] recently reported that the leakage current in BFO ceramics is the space-charge-limited current (SCLC). Therefore, the further study of the leakage mechanism and the influence on the electrical reliability of BFO ceramics is still necessary.

In this letter, we present the well saturated polarization loops in highly resistive La$_{0.1}$Bi$_{0.9}$FeO$_3$ (LBFO) ceramics at room temperature, and furthermore the leakage mechanisms in the LBFO ceramics and their influence on the electrical reliability are investigated.

The single-phase LBFO ceramics were prepared by a modified rapid sintering process (MRSP).[8,9] High purity (99.99%) starting powders of Bi$_2$O$_3$, Fe$_2$O$_3$, and La$_2$O$_3$ were weighed according to the stoichiometric composition. These weighted powders were mixed in agate mortars with alcohol and milled for 5 h. After drying, these homogeneous mixtures were calcined at 830–860 °C for 3 h. To obtain ceramics, the calcined powder was hydrostatically cold pressed into 0.4 mm thick disks. Then, by using a high heating and cooling rate of about 100 °C/s, these pressed disks were sintered at 830–860 °C for 30 min in air.

The crystalline structure of the ceramics was examined by x-ray diffractometer (Rigaku D-max 2500 PC) using Cu K_α radiation. For the measurement of electrical properties, both surfaces of the ceramic disks were polished and coated with silver paste as electrodes. Dielectric measurement was performed by using WK 3410 precision impedance analyzer. Leakage current, P-E loops, electrical reliability were measured with an Aixacct model TF 2000 ferroelectric analyzer.

The relative density of ~90% is obtained for the sintered LBFO ceramics. The x-ray diffraction (XRD) patterns of the ceramics were shown in Fig. 1. The XRD results indicate no

a)Author to whom correspondence should be addressed. Tel.: +8615822652429. FAX: +862223766519. Electronic mail: shouyu.wang@yahoo.com.
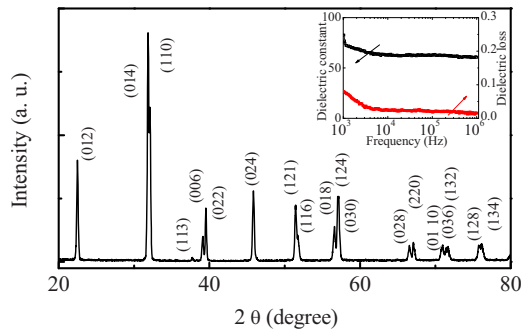
98, 152902-1

FIG. 1. (Color online) X-ray diffraction pattern of $La_{0.1}Bi_{0.9}FeO_3$ ceramic. The Bragg reflections are indexed. Inset shows the dielectric constant and the dielectric loss of the ceramic as a function of the frequency.

traces of impurity phases in the LBFO ceramic samples. The XRD profile shows split reflections at $2\theta = 39.5°$ and $57.2°$, which indicating a rhombohedral structure in $La_{0.1}Bi_{0.9}FeO_3$ ceramic.[17] The variation in the dielectric constant and the dielectric loss as a function of frequency for the LBFO ceramic is shown in the inset of Fig. 1. With the increase in the frequency from 1 kHz to 1 MHz, the dielectric constant decreases slowly from 75.1 to 53.2 and the dielectric loss decreases from 7.7% to 1.6%.

Figures 2(a) and 2(b) show the displacement currents and polarization loops of the LBFO capacitor under various driving electric field, respectively. As the applied electric field is ramped to around $70–75$ kV cm^{-1} s^{-1}, the displacement currents exhibit a sharp increase, demonstrating the occurrence of polarization switching in the LBFO ceramics, as shown in Fig. 2(a). An applied electric field can lead to a change in the surface charges of the sample. One contribution is from the ferroelectric domain switching which can be represented by the sharp increase in the displacement currents $J_D (= dD/dt)$. As the polarization dynamics cease after a certain time, J_D subsides, and further change in the surface charge can be attributed to leakage currents through the sample, which will be discussed in the later part. If the LBFO sample is not highly resistive and the leakage currents are large to overlay the domain switching current, the sharp increases in the displacement current cannot be observed. Therefore, the observed domain switching current indicates low leakage current in the LBFO ceramics. The forward and backward coercive electric fields can be determined from the
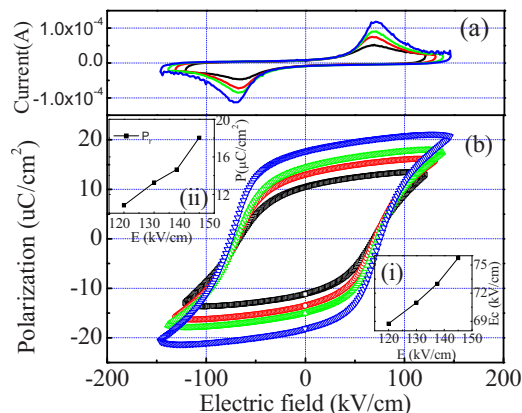

FIG. 2. (Color online) Displacement current (a) and ferroelectric polarization (b) vs electric field as measured at room temperature at a measuring frequency of 10 Hz. Inset (i) and (ii) show the coercive field and polarization values as a function of biased electric field, respectively.
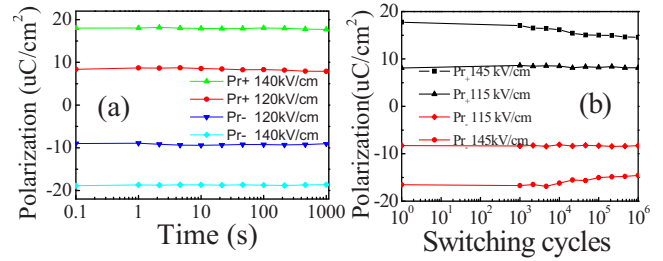

FIG. 3. (Color online) Polarization retention (a) and fatigue traits (b) of the LBFO ceramic.

current peak position (maximum current), which increases with the driving electric field, as shown in the inset (i) of Fig. 2. Moreover, the room temperature P-E response shows a well square hysteresis loops. The remanent polarization (P_r) increases with the maximum driving electric field, as shown in the inset (ii) of Fig. 2. When the maximum driving filed is 145 kV/cm, the measured values of the remanent polarization and the coercive field are 17.8 $\mu C/cm^2$ and 75 kV/cm, respectively. The remanent polarization obtained in the LBFO ceramics is significantly larger than those of some bulk ceramics and single crystal,[8–11,18–20] though it is less than those of epitaxial thin films.[1,2,4,6] Such a large remanent polarization in our polycrystalline ceramic is comparable to that of the $BiFeO_3$ ceramics prepared by high-pressure synthesis.[10]

Figure 3(a) shows the retention of the remanent polarization of the LBFO capacitor after poling with 120 and 140 kV/cm. It can be seen that the remanent polarization does not show obvious degradation after 1000 s. Figure 3(b) shows the fatigue characteristic of the LBFO ceramic sample measured at a switching frequency of 1 kHz and electric fields of ± 145 and ± 115 kV/cm. It can be seen that, after being subjected to 10^6 switching cycles at 115 kV/cm, there is no obvious degradation in the remanent polarization; However, for electric field of 145 kV/cm, the remanent polarization shows a decrease of 17% (from 17.7 to 14.5 $\mu C/cm^2$). It was reported that the remanent polarization decreases more than 50% only after 18 electric cycles in $BiFeO_3$ single crystal sample, which was ascribed to the Joule heating effect induced by larger leakage current during full saturation cycles.[7]

Figure 4(a) shows the leakage current density versus bias electric field (J-E) up to ± 150 kV/cm. In order to determine the leakage mechanism, J-E characteristics on a logarithmic scale and the differential curve of the log(J) versus log(E) are also plotted in Fig. 4(a). In the region of E < 75 kV/cm, the slope is around 1.0, thus the leakage current follows Ohmic law. In the region of 75 kV/cm < E < 150 kV/cm, the slope varies from 5.0 to 2.0, indicating that the conduction mechanism may be Schottky emission, the Pool–Fenkel emission mechanism[11,14,21] or the SCLC.[15,17]

The current density for the Schottky emission can be expressed as follows:[21]

$$J_S = AT^2 \exp\left[\frac{q(\sqrt{qV/4\pi\varepsilon_0\varepsilon_{or}d} - \Phi)}{k_B T}\right], \tag{1}$$

where A is the Richardson constant, Φ is the height of the Schottky barrier, k_B is the Boltzmann constant, T is the temperature in Kelvin, ε_{or} is the optical dielectric constant of the ceramic, and d is the sample thickness. For the Poole–
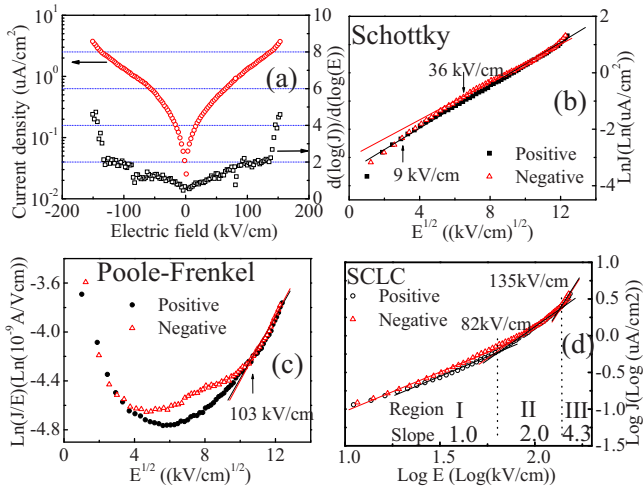
FIG. 4. (Color online) Typical J-E characteristics of the La$_{0.1}$Bi$_{0.9}$FeO$_3$ ceramics at room temperature. (a) J-E characteristics on a logarithmic scale and the slope of the log(j) vs log(e) curve. Various fits of the leakage current data are shown to help determine the leakage mechanism: (b) Schottky emission, (c) Poole–Frenkel emission, or (d) SCLC.

Frenkel mechanism dominated current, J_{PF} can be expressed as follows:[21]

$$J_{PF} = cE \exp\left[\frac{q\sqrt{qV/\pi\varepsilon_0\varepsilon_{or}d} - E_t}{k_B T} \right], \quad (2)$$

where c is a constant, and E_t is the trap ionization energy.

Leakage current data for both positive and negative biases are plotted in the same scales with mentioned mechanisms, as shown Fig. 4. When the $E > 9$ kV/cm for positive bias or $E < -36$ kV/cm for negative bias, the results can be fitted well with the Schottky equation as shown by the straight line in Fig. 4(b). When the $E > 103$ kV/cm for positive bias or $E < -103$ kV/cm for negative bias, the Poole–Frenkel mechanism also provides a good fit, as shown in Fig. 4(c). The slope of the fit lines provides an estimation of the optical dielectric constant ε_{or}, and ε_{or} is thereby estimated as 0.67 and 1.56 for Schottky emission and Poole–Frenkel, respectively. These dielectric values are not in agreement with the optically determined value of about 6.25.[14,22] Therefore, at high electric field, the leakage current in the LBFO cannot be described with the Schottky emission or Poole–Frenkel leakage mechanism.

Figure 4(d) shows a plot of the log(J) versus log(E) for positive and negative bias. According to the slope, each curve can be divided into three regions. Such characteristics agree well with the SCLC theory with deep traps.[16] The region I follows the Ohmic law. The region II corresponds to the trap-filling process characterized by a slope of 2.0. After the accomplishment of trap-filling, the leakage current gives a sharp increase. The conduction current in region II can be expressed as follow:[16]

$$J_{SCLC} = \frac{9\mu_p\varepsilon_r\varepsilon_0\theta E^2}{8d}, \quad (3)$$

where E is the bias electric field, ε_r is the permittivity of the ceramic, μ_p is the mobility of the charge carriers, and θ is the ratio of the total density of the induced free carriers to the trapped carriers.

For our LBFO ceramics, the MRSP may reduce the formation of charged defects, such as Fe^{2+} ions, V$_{Bi}^{2+}$ vacan-

cies, and V$_O^{2+}$ vacancies in the samples.[11,18–20,23,24] The low density of defects is a key factor to get the low leakage current and the well saturated ferroelectric hysteresis loops. However, in polycrystalline ceramic, there are still two charge-transfer bands and some traps level associating with the defects in the band gap.[15] The V$_O^{2+}$ vacancies act mainly as the internal traps in the polycrystalline samples, and they can move through the sample under electric fields as positive mobile charge.[4,11] The charged defects, especially oxygen vacancy in LBFO ceramic could pin the ferroelectric domain wall, resulting in the decreasing of polarization during electrical switching process.

In summary, high resistive LBFO ceramics were synthesized with the MRSP method. Low leakage current, well saturated polarization loops, and excellent electrical reliability were obtained in the LBFO ceramics. The electrical conduction in the ceramics has been found to be controlled by SCLC rather than the thermal excitation mechanisms.

[1]S.-W. Cheong and M. Mostovoy, Nature Mater. **6**, 13 (2007).
[2]R. Ramesh and N. A. Spaldin, Nature Mater. **6**, 21 (2007).
[3]T. Choi, S. Lee, Y. J. Choi, V. Kiryukhin, and S.-W. Cheong, Science **324**, 63 (2009).
[4]C.-H. Yang, J. Seidel, S. Y. Kim, P. B. Rossen, P. Yu, M. Gajek, Y. H. Chu, L. W. Martin, M. B. Holcomb, Q. He, P. Maksymovych, N. Balke, S. V. Kalinin, A. P. Baddorf, S. R. Basu, M. L. Scullin, and R. Ramesh, Nature Mater. **8**, 485 (2009).
[5]J. B. Neaton, C. Ederer, U. V. Waghmare, N. A. Spaldin, and K. M. Rabe, Phys. Rev. B **71**, 014113 (2005).
[6]J. Wang, J. B. Neaton, H. Zheng, V. Nagarajan, S. B. Ogate, B. Liu, D. Viehland, V. Vaithyanathan, D. G. Shlom, U. V. Wahgmare, N. A. Spaldin, K. M. Rabe, M. Wuttig, and R. Ramesh, Science **299**, 1719 (2003).
[7]D. Lebeugle, D. Colson, A. Forget, and M. Viret, Appl. Phys. Lett. **91**, 022907 (2007).
[8]S. T. Zhang, M. H. Lu, D. Wu, Y. F. Chen, and N. B. Ming, Appl. Phys. Lett. **87**, 262907 (2005).
[9]S. T. Zhang, Y. Zhang, M. H. Lu, C. L. Du, Y. F. Chen, Z. G. Liu, Y. Y. Zhu, N. B. Ming, and X. Q. Pan, Appl. Phys. Lett. **88**, 162901 (2006).
[10]W. N. Su, D. H. Wang, Q. Q. Cao, Z. D. Han, J. Yin, J. R. Zhang, and Y. W. Du, Appl. Phys. Lett. **91**, 092905 (2007).
[11]G. L. Yuan, and S. W. Or, Appl. Phys. Lett. **88**, 062905 (2006).
[12]J. M. Liu, F. Gao, G. L. Yuan, Y. Wang, M. Zeng, and J. G. Wan, J. Electroceram. **21**, 78 (2008).
[13]A. Morelli, S. Venkatesan, G. Palasantzas, B. J. Kooi, and J. T. M. De Hosson, J. Appl. Phys. **102**, 084103 (2007).
[14]G. W. Pabst, L. W. Martin, Y.-H. Chu, and R. Ramesh, Appl. Phys. Lett. **90**, 072902 (2007).
[15]B. Ramachandran, A. Dixit, R. Naik, G. Lawes, and M. S. Ramachandra Rao, Phys. Rev. B **82**, 012102 (2010).
[16]M. A. Lampert and P. Mark, *Current Injection in Solids* (Academic, New York, 1970).
[17]A. V. Zalesskii, A. A. Frolov, T. A. Khimich, and A. A. Bush, Phys. Solid State **45**, 141 (2003).
[18]Y. P. Wang, L. Zhou, M. F. Zhang, X. Y. Chen, J.-M. Liu, and Z. G. Liu, Appl. Phys. Lett. **84**, 1731 (2004).
[19]B. F. Yu, M. Y. Li, J. Wang, L. Pei, D. Y. Guo, and X. Z. Zhao, J. Phys. D **41**, 185401 (2008).
[20]Y. Wang and C. W. Nan, Appl. Phys. Lett. **89**, 052903 (2006).
[21]S. M. Sze, *Physics of Semiconductor Devices*, 2nd ed. (Wiley, New York, 1981).
[22]S. Iakovlev, C.-H. Solterbeck, M. Kuhnke, and M. Es-Souni, J. Appl. Phys. **97**, 094901 (2005).
[23]M. Kumar and K. L. Yadav, Appl. Phys. Lett. **91**, 242901 (2007).
[24]D. K. Pradhan, R. N. P. Choudhary, C. Rinaldi, and R. S. Katiyar, J. Appl. Phys. **106**, 024102 (2009).